Preprints.org

Article

Combined Impacts of Rainfall Patterns and Intensive Tillage Erosion on Soil and Water Loss in a Simulated Tillage-Eroded Area

Yong Wang [*] , Yunlian Jin , Jiaqi Wang , Zhenzhen Ma , Xing Liu , Xinlan Liang

Article

Combined Impacts of Rainfall Patterns and Intensive Tillage Erosion on Soil and Water Loss in a Simulated Tillage-Eroded Area

Yong Wang [1,2], Yunlian Jin [1], Jiaqi Wang [1], Zhenzhen Ma [1], Xing Liu [3] and Xinlan Liang [3,*]

[1] College of Forestry, Sichuan Agricultural University, Chengdu 611130, China
[2] Key Laboratory of Soil and Water Conservation and Desertification Combating, Sichuan Agricultural University, Chengdu 611130, China
[3] College of Water Conservancy and Hydropower Engineering, Sichuan Agricultural University, Ya'an 625014, China
[*] Correspondence: Correspondence: wysoil@126.com

Abstract: Many studies have focused on the impacts of rainfall duration and intensity while overlooking the role of rainfall patterns on intensive tillage erosion in hilly agricultural landscapes. The objective of this study was to determine the combined effects of rainfall patterns and intensive tillage erosion on surface runoff and soil loss on sloping farmland in the purple-soil area of China. Five simulated rainfall patterns (constant, rising, falling, rising-falling, and falling-rising) with the same total precipitation were designed, and the intensive tillage erosion treatment (IT) and no-tillage treatment (NT) were subjected to simulated rainfall using rectangular steel tanks (2 m × 5 m) with a slope of 15°. To analyse the differences in the hydrodynamic characteristics induced by tillage erosion, we calculated the flow velocity (V), Reynolds number (Re), Froude number (Fr), and Darcy-Weisbach resistance coefficient (f). The results indicate that significant differences in surface runoff and soil loss were found among different rainfall patterns and stages ($P < 0.05$). The falling pattern and falling-rising pattern had faster runoff-initiating times and larger sediment yields than those of the other rainfall patterns. f varied from 0.30 to 9.05 for the IT and 0.48 to 11.57 for the NT and exhibited an approximately inverse trend to V and Fr over the course of the rainfall events. Compared with the NT, the mean sediment yield rates from the IT increased the dynamic range of 8.34%–16.21% among different rainfall patterns. The net contributions of the IT ranged from 2.77% to 46.39% on surface runoff and 10.14%–78.95% on soil loss on sloping farmland. Surface runoff and soil loss were positively correlated with rainfall intensity, V, and Fr but negatively correlated with f irrespective of tillage intensive ($P < 0.05$). For varying-intensity rainfall patterns, soil and water loss fluctuated during rainfall events, suggesting that the changes in rainfall intensity and tillage intensity would result in drastic variations in soil hydrological characteristics and sediment transport mechanisms. The time sequences of rainfall intensity in each rainfall pattern significantly affected surface runoff, soil erosion, and their contribution rates to total soil and water loss. Moreover, tillage erosion effects on soil and water loss were closely related to rainfall patterns in hilly agricultural landscapes. Our study not only sheds light on the mechanism of tillage erosion and rainfall erosion but also provides useful insights for developing tillage-water erosion prediction models to evaluate soil and water loss on cultivated hillslopes.

Keywords: tillage operation; rainfall pattern; hydrological characteristics; surface rainfall; soil loss

1. Introduction

Soil and water loss continues to be a serious threat in many cultivated agricultural lands, and it results in reduced crop production and environmental degradation. Natural rainfall is a crucial driving force that governs surface runoff and soil loss processes. The properties of rainfall, such as intensity, interval, and duration, are critical factors that impact the processes of surface runoff and soil erosion [1–3]. The intensity of rainfall fluctuates greatly over time, and the maximum rates of precipitation can surpass the average rate by up to ten times [4, 5]. Under natural rainstorms, a series of field experiments by Mohamadi and Kavian (2016) revealed that storms with increasing rainfall intensity produced the most soil and water loss [6]. For the typical black soil region of Northeast China, the soil loss for the rising-falling pattern was 1.20, 1.63, 1.78, and 1.80 times higher than those

of the falling-rising, falling, constant, and rising patterns, respectively [7]. An et al. (2017) compared four different rainfall patterns in cinnamon soil and concluded that surface runoff was ranked in the following order for various storm patterns: falling-rising > falling > rising-falling > rising patterns [8]. Different rainfall patterns and rainfall stages have significant differences in soil and water loss [2, 4, 9]. These studies demonstrate that different rainfall patterns have essential influences on surface runoff and sediment yield on cultivated hillslopes.

Although variable rainfall intensity is a common phenomenon during natural rainfall events, there are serious inadequacies in the study of the effect of variable rainfall intensity combinations (rainfall patterns) on the soil loss process in hilly croplands, especially under the conditions of intensive tillage erosion. In agricultural fields, the influence of different rainfall intensities on the processes of soil and water loss is largely related to tillage operations [10]. Previous studies have demonstrated that tillage erosion results in soil translocation on hillslopes, and the processes of tillage operations result in soil movement downslope, leading to soil accumulation in lower slope positions and decreased soil in higher slope positions [11, 12]. Tillage-induced progressive soil redistribution significantly affects soil hydrological properties and rainfall-runoff processes, as it alters soil profile properties, such as soil structure and layer thickness, within the landscape [13, 14].

The thickness of the soil layer is an important factor that strongly affects runoff and hydrodynamic processes in agricultural landscapes. A thin soil layer can result in higher erosion rates due to the direct exposure of underlying rock and soil, thus increasing soil susceptibility to mechanical stresses and weathering processes [15, 16]. In addition, a thin soil layer can decrease water infiltration and retention, which then enhances runoff and sediment yield [17, 18]. These studies have shown that soil thickness is a key factor controlling soil and water loss, as it can strongly influence soil properties and hydrological processes. However, there is still limited research on the impact of soil thickness caused by long-term tillage erosion on soil and water loss, especially under different rainfall conditions.

In the hilly areas of Sichuan, there has been a long history of tillage operations due to the high population density and land deficiency. Farmers traditionally till their fields twice a year to loosen the surface soil, improve the soil physical properties, and increase land productivity. Furthermore, the rainfall intensity in this region is relatively high, and the variation process of rainfall is complex. As a result, the combination of intensive tillage erosion and rainfall erosion result in extremely severe soil and water loss. However, studies have proven that tillage erosion and rainfall erosion are the main causes of soil loss in the hilly areas of the Sichuan Basin [12]. Although there are many descriptive comments and viewpoints on the relationship between tillage operation and soil and water loss in sloping fields, how the combination of rainfall patterns and intensive tillage affect runoff and soil erosion remains unresolved. Against this background, the objectives of this study were to (1) analyse the changes in surface runoff and sediment yield rate for different tillage erosion intensities with different rainfall patterns; (2) determine the interactions of varied rainfall intensity, stage, and intensity sequence under intensive tillage and no-tillage operations; and (3) examine the hydrologic mechanisms between different tillage intensities under different rainfall patterns in the purple soil region.

2. Materials and Methods

2.1. Study sites and experimental design

Soil samples were gathered from a representative area of the purple soil region located in Mingshan District, Ya'an city, Sichuan Province, Southwest China (29°57'36"–30°16'15"N, 103°2'40"–103°24'01"E). This area is dominated by a subtropical humid monsoon climate. The study area experiences a subtropical monsoon humid climate, with a mean annual temperature of 16 °C and approximately 1500 mm of precipitation that is distributed unevenly throughout the year. Most rainstorms occur from May to October, when a heavy rainfall intensity greater than 100 mm h^{-1} is usual. The soils found in this area, originating from purple mudstone deposits from the Jurassic Age, have been classified as Orthents [19]. The farmland had been cultivated successively for over 50 years, thereby resulting in a shallow soil depth due to long-term tillage operations and water erosion effects. The corrosion resistance of the soils is poor. Table 1 provides a summary of the soil properties, and Liu (1996) provides a detailed description of the sampling and determination methods used [20]. The soil tested in this experiment had a bulk density of 1.44 g cm^{-3} with an average of 42.62% clay (<0.002

mm), 28.33% silt (0.002–0.02 mm) and 29.05% sand (0.02–2 mm). The soil organic carbon (SOC) content was 10.71 g kg^{-1}.

Table 1. The measured properties of the soils in the study.

Soil property	Minimum	Maximum	Mean	SD	CV (%)
Sand (%)	24.54	34.71	29.05	4.23	14.56
Silt (%)	21.04	36.57	28.33	6.41	22.63
Clay (%)	37.13	46.53	42.62	4.10	9.63
Bulk density (g cm^{-3})	1.21	1.58	1.44	0.16	11.04
Soil depth (m)	0.36	0.48	0.43	0.05	11.86
Total porosity	0.44	0.51	0.47	0.03	6.73
Soil water content (%)	14.27	20.75	17.58	2.66	15.14
pH	7.81	8.40	8.11	0.25	3.04
SOC (g kg^{-1})	5.73	7.57	6.21	0.91	14.58
Total N (g kg^{-1})	0.82	1.15	0.93	0.15	16.16
CaCO3 (g kg^{-1})	83.6	103.76	93.97	8.24	8.77

The soil samples (0–0.30 m depth) collected in the field were air dried, and the roots, stones and other debris were removed. Then, the soil blocks were crushed into fine soil particles and infilled into two neighbouring steel tanks (2 m in width, 0.45 m in depth, and 5 m in length) through a 0.01m sieve with an infilling depth of 0.40 m. Before infilling the soil, a layer of permeable board approximately 0.02 m was laid at the bottom of the steel tank, and the permeable board was provided with a permeable hole with a diameter of 0.01 m and an interval of 0.01 m. A layer of cotton gauze was laid above the board to ensure the permeability and prevent soil particles from leaking from the permeable board.

Intense tillage erosion in the hilly areas of the Sichuan Basin often result in shallow soil depths, and in some cases, bedrock is even exposed on the summits of agricultural land. Previous literature based on field investigations has revealed that the soil profile at the upslope boundary has completely disappeared, leading to bedrock exposure due to intensive tillage [17, 21, 22]. Based on field surveys and previous studies, we covered a piece of plastic sheet (1 m long and 2 m wide) in the soil surface of one steel tank at the summit position (1−2 m) to simulate bedrock exposure, this scenario represented the intensive tillage erosion treatment (IT), and erosion rate reached 129.60 Mg ha^{-1}. In contrast, another steel tank without a cover was considered the no-tillage treatment (NT, Figure 1a).

Figure 1. Different tillage intensity treatments (a) and Rainfall simulation (b).

2.2. Rainfall simulation

Artificial rainfall events were performed at Sichuan Agricultural University located in Ya'an city, Sichuan Province, China. The rainfall simulator (Model: NLJY-10-03) is a portable fully automatic simulator with a series of stainless steel pipes and down-sprayers made by Nanlin Electronics Technology Incorporation. The rainfall simulation device used was similar to the one described by Dai et al. (2017) [23], whose effective rainfall area was 10 m × 6 m and had a sprayer at a height that was 6 m above the ground (Figure 1b). Therefore, the rainfall area was sufficient to cover the area of the two neighbouring steel tanks in the experiment. It was possible to manually adjust the rainfall intensity within a range of 15 to 240 mm h^{-1}, with a raindrop distribution uniformity of over 85%. A hole with a 0.04 m aperture was located at the bottom edge of the steel tank to ensure free drainage during rainfall. The slope steepness of the steel tank could be adjusted within a range of 0–30°; however, for our tests, we chose a slope of 15°, as the experimental region has a threshold gradient that determines the conversion of farmland to grassland or forestland.

To minimize experimental errors caused by the variable rainfall intensities during rainfall simulation and to represent natural conditions, we designed five different rainfall patterns based on field surveys and literature analysis [2, 24]: constant pattern (rainfall intensity distribution with 90

mm h^{-1}, CR), rising pattern (rainfall intensity sequence as 30–60–90–120–150 mm h^{-1}, RR), falling pattern (rainfall intensity sequence as 150–120–90–60–30 mm h^{-1}, FR), rising-falling pattern (rainfall intensity sequence as 30–90–150–90–30 mm h^{-1}, RFR), and falling-rising pattern (rainfall intensity sequence as 150–90–30–90–150 mm h^{-1}, FRR). Each rainfall pattern was carried out with the same total rainfall of 90 mm and was divided into 5 periods (Figure 2a–e), each corresponding to a specific rainfall intensity.
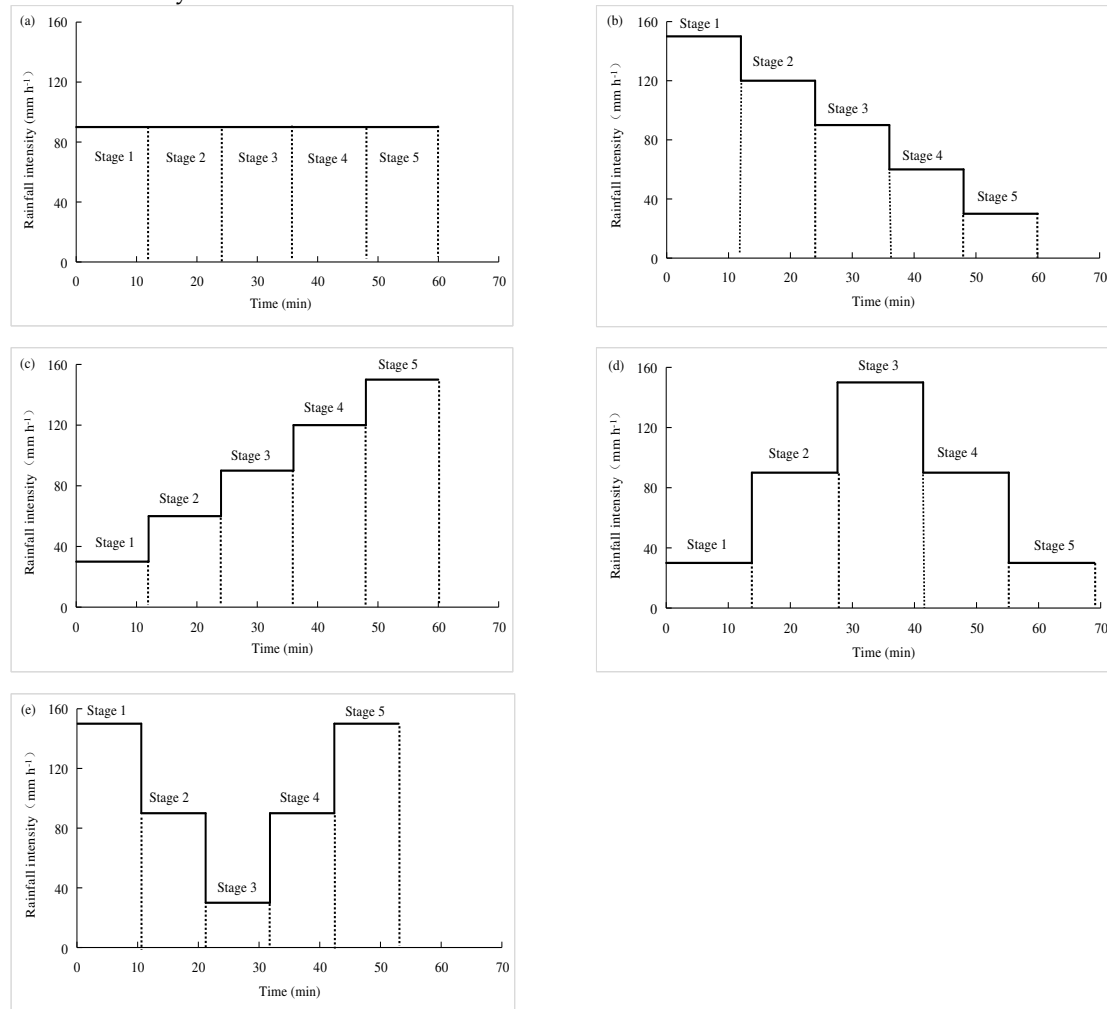
Figure 2. Rainfall patterns for the simulated rainfall: (a) constant pattern, (b) falling pattern, (c) rising pattern, (d) rising–falling pattern, and (e) falling–rising pattern.

To ensure that the soil moisture content was consistent before each rainfall event, pre-rainfall was carried out before each rainfall event, and the soil moisture content was measured with a portable soil moisture analyser to control the soil moisture content between 25% and 30%. At the beginning of the simulated rainfall, the runoff initiation time was recorded when the runoff began to flow from the outlet of the steel tank. We continuously collected surface runoff and sediment samples in pre-weighed plastic buckets every 2 minutes. The excess water was poured away after 24 h of precipitation, and the sediment was poured into an aluminium box and dried in the oven at 105 ℃. The samples were then weighed again to calculate the runoff amount, sediment discharge and cumulative infiltration volume (mm). Surface flow velocity was measured using K_2MnO_4 colouration for each rainfall stage on the upper, middle, and lower slope positions. The upper slope was from the top to shoulder positions (0–1 m), the middle slope was from the shoulder to middle positions (2–3 m), and the lower slope was from the middle to the outlet (4–5 m). The mean flow velocity (V) was obtained by multiplying the surface flow velocity with a correction coefficient of 0.67 according to a previous study [25]. The time taken for the tracer to travel a marked distance of 1 m was determined by analysing the propagation of the colour front using a stop-match method. To analyse the hydraulic characteristics of the flow, calculations were performed to determine the Reynolds number (Re),

Froude number (*Fr*), and Darcy-Weisbach resistance coefficient (*f*). The formulas for calculating these parameters can be found in [26].

2.3. Statistical analysis

A paired t test was conducted using SPSS 26.0 software to examine statistically significant differences in the surface runoff and sediment yield between the IT and NT treatments under different rainfall patterns. SigmaPlot 14.0 software was used to fit the equations of runoff rate and sediment yield rate. Meanwhile, AMOS 21.0 software was used to analyse the correlations between the rainfall intensity, surface runoff rate, hydrologic parameters and sediment yield rate under the IT and NT treatments using a structural equation model (SEM). Redundancy analysis (RDA) using Canoco 5 software was used to check the effects of different hydraulic characteristic variables on runoff amount and sediment yield.

3. Results

3.1. Responses of runoff rates and sediment yield to tillage erosion and rainfall patterns

The runoff-initiating time in the IT and NT treatments for different rainfall patterns are depicted in Figure 3. During the rainfall event with a total of 90 mm rainfall, a noticeable difference in runoff rates was observed among different rainfall patterns. Additionally, the time gap between runoff occurrence and rainfall initiation varied mainly depending on the rainfall pattern. As shown in Figure 3, the runoff-initiating time for IT was earlier than that for NT under the same rainfall patterns. The longest runoff-initiating time was observed in NT, whereas the shortest time was found in NT for the same rainfall pattern. In both tillage treatments, the order of the time to runoff initiation was RR > RFR > CR > FRR > FR. FR and FRR had faster runoff-initiating times than those of the other rainfall patterns. Compared with no-tillage, the runoff-initiating time for intensive tillage increased by 10.03%, 33.68%, 16.42%, 6.32%, and 33.82% for RR, FR, CR, RFR, and FRR, respectively. Runoff generation from FR and FRR was faster than that of other rainfall patterns. These results indicated that surface runoff was more likely to occur on the intensively tilled soils, and the presence of soil thickness induced by tillage operation seemed to be the main factor that delayed the initial runoff generation time.
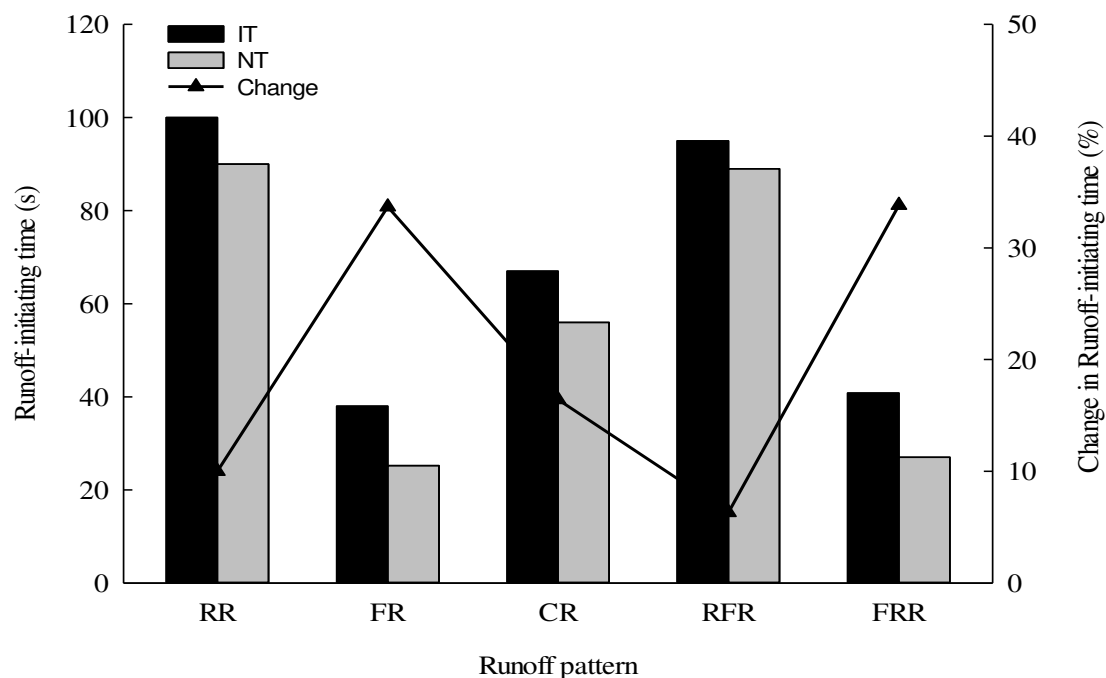

Figure 3. Initial production flow time of different rain patterns. Note: IT means intensive tillage treatment; NT means no-tillage treatment.

3.2. Effect of tillage erosion on surface runoff rate and runoff volume

As shown in Figure 4, the surface runoff rate for the two tillage treatments had a similar trend under different rainfall patterns. The change trend of the surface runoff rate in each stage of the rainfall pattern was consistent with that of the rainfall intensity for different rainfall patterns, yet the surface runoff rate under NT first increased sharply and then stabilized gradually as rainfall duration increased. Lower runoff rates were found in the RFR patterns than in the other rainfall patterns for the two treatments. Figure 4 shows the peak runoff rates for the different rainfall patterns, which were statistically 1.55 to 1.60 and 1.67 to 1.78 times greater than the peak runoff rate for the CR pattern for NT and IT, respectively. Regardless of tillage intensity, the study found that the peak runoff rates during rainfall with varying intensities were significantly higher than those observed during storms with constant intensity. These results suggest that the tillage intensity may influence the relationship between the peak runoff rate and the rainfall pattern.

Significant differences by paired t test were found in the cumulative runoff volume for the rainfall patterns between NT and IT (P = 0.005), implying that the significant influence of different rainfall patterns on sediment yield was closely related to tillage intensity. The cumulative runoff volume varied from 551.89 to 642.16 L and 641.35 to 706.72 L for NT and IT during the rainfall event, respectively. The cumulative runoff volume for the two tillage treatments increased as follows: FR < RFR < RR < CR < FRR, and the cumulative runoff volume resulting from the different rainfall patterns in the IT treatment was higher than that in the NT treatment. These results suggest that the cumulative runoff volume was impacted by the different rainfall patterns and tillage intensities.
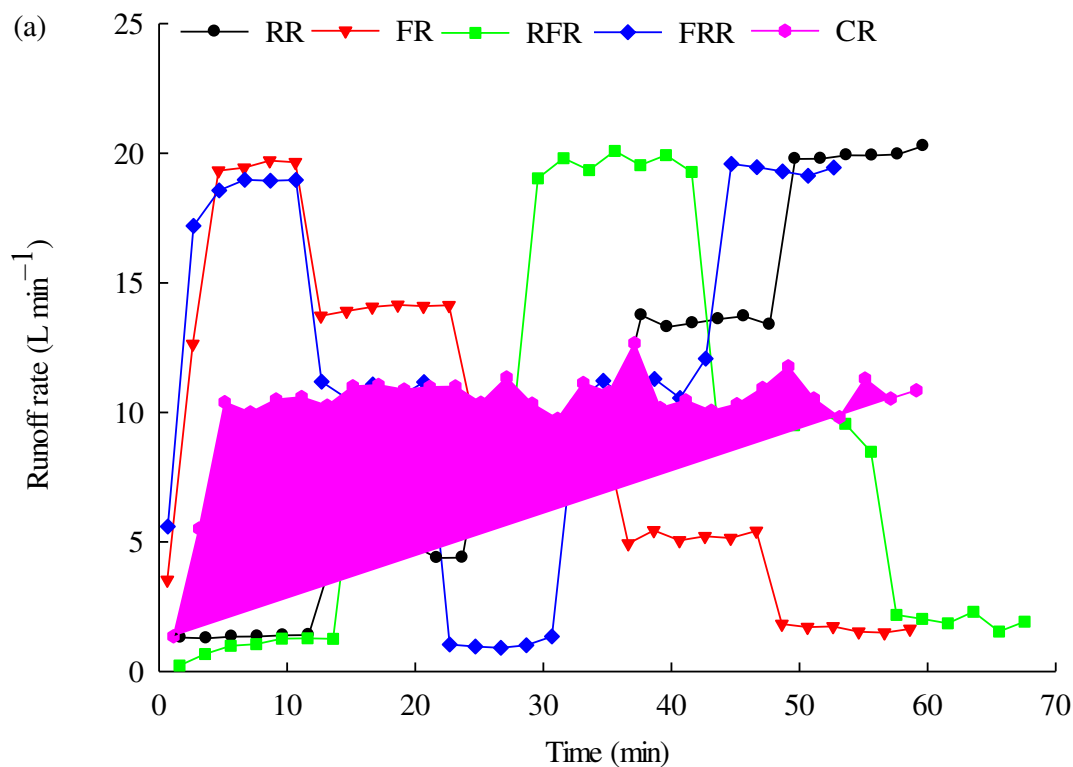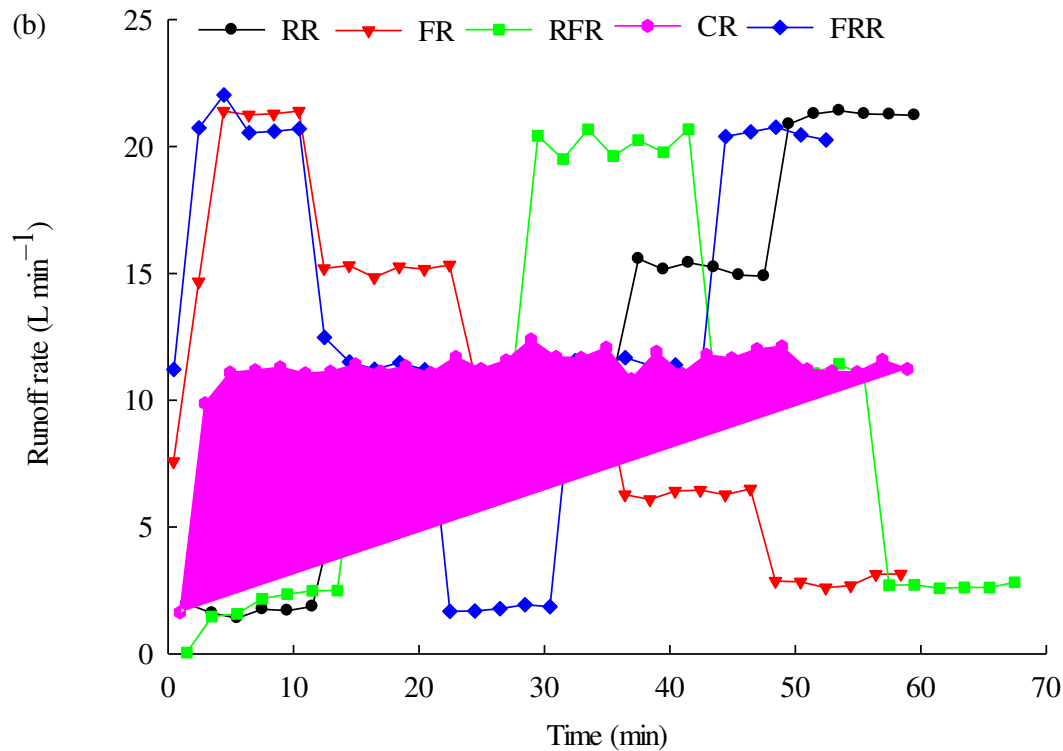
Figure 4. Temporal variations of runoff rate under different rainfall patterns. (a) NT, (b) IT.

3.3. Changes in soil loss and sediment concentration under different rainfall patterns

Figure 5 illustrates the temporal changes in sediment yield rates under different rainfall patterns. Generally, sediment yield rates exhibit changes based on the rainfall intensity during the rainfall event. The temporal trend of sediment concentration varied significantly across all rainfall patterns and tillage intensities. For the CR pattern, the sediment yield rate for both IT and NT increased sharply at the beginning and then decreased gradually, remaining stable until the end of the rainfall event. However, for the other four rainfall patterns, the sediment yield rates were inconsistent at different stages, despite having the same average rainfall intensity per storm. The sediment yield rates for IT ranged from 1.41 to 21.42 L min^{-1}, 2.61 to 21.40 L min^{-1}, 0.05 to 20.69 L min^{-1}, 1.68 to 22.04 L min^{-1}, and 1.63 to 12.40 L min^{-1} for RR, FR, RFR, FRR, and CR, respectively. A similar range of sediment yield rates was observed in different rainfall patterns for NT. Compared to that for NT, the mean sediment yield rates for IT increased by 8.34%–16.21%, with an average of 11.59% under different rainfall patterns. These findings suggest that the sediment yield rate displayed a rapid and obvious response to rainfall patterns and tillage intensities.
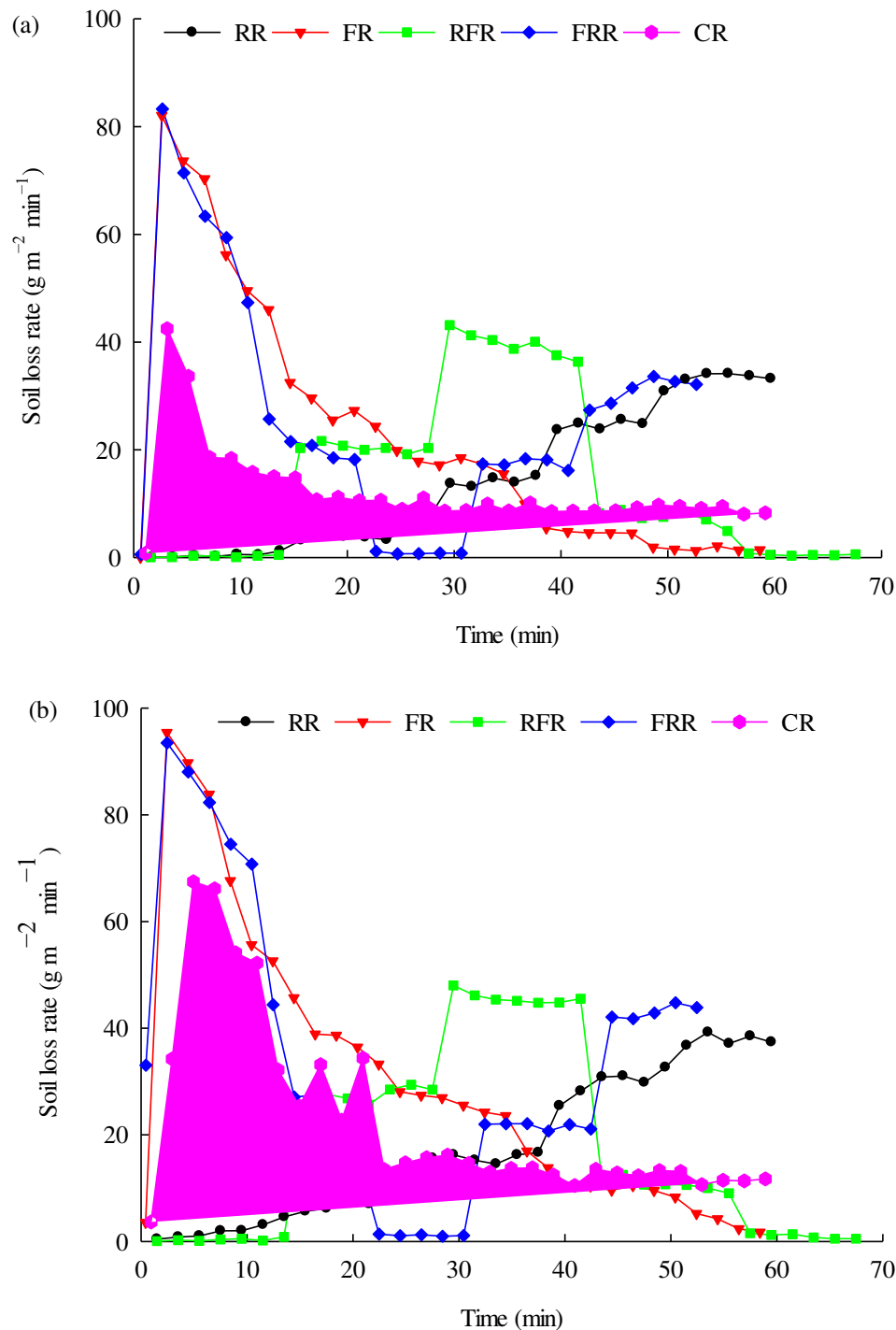
Figure 5. Temporal variations of soil loss rates under different rainfall patterns. (a) NT, (b) IT.

The cumulative sediment production is ranked as FRR > FR > RFR > RR > CR and FRR > FR > RFR> CR > RR for NT and IT, respectively. Regardless of the NT and IT treatments, the cumulative sediment production under FR and FRR was higher than that from the other rainfall patterns in both NT and IT, showing that the early stages of the short high-intensity rainfall events had a critical impact on soil loss on steep slopes. There was a significant difference ($P = 0.008$) in the cumulative sediment production between the NT and IT treatments. The cumulative sediment production for the NT treatment reached 8.57, 13.34, 7.33, 9.54, and 13.20 kg for RR, FR, CR, RFR, and FRR, respectively. Compared with the NT, the cumulative sediment production from IT increased by 21.69%, 35.03%, 83.95%, 24.85%, and 40.70% for RR, FR, CR, RFR, and FRR, respectively, indicating that the sediment concentration significantly improved after intensive tillage in a hilly landscape.

3.4. Impacts of rainfall patterns and tillage erosion on hydraulic characteristics

The hydraulic parameters, such as V, Re, Fr, and f, for different rainfall patterns and tillage intensities during the rainfall events, are presented in Table 2. The mean V, Re, and Fr values ranged from 6.03 to 19.36 cm/s (5.45 to 14.69 cm/s), 78.35 to 137.23 (62.95 to 122.93), and 0.48 to 2.64 (0.42 to 2.09) for storms under the IT (NT) treatment, respectively. The trends of V and Fr showed a more pronounced increase over time in comparison to the rainfall pattern experiment, indicating that rainfall stage had a stronger impact on V and Fr. However, this trend was weaker in Re. f varied from 0.30 to 9.05 for IT and from 0.48 to 11.57 for NT and exhibited an approximately inverse trend to V and Fr over the course of the rainfall experiments. The hydrodynamic parameters showed a general increase with increasing rainfall intensity, but no significant differences were found in V, Re, and Fr among the different rainfall stages and patterns at each rainfall intensity. A significant difference in hydrodynamic parameters was found between IT and NT for each rainfall event ($P < 0.01$). In addition, Table 2 shows that the V, Re, and Fr resulting from the different rainfall patterns and stages in IT were greater than those in NT. The results indicate that long-term tillage had an important effect on hydraulic parameters under the same rainfall conditions.

Table 2. Hydraulic parameters under different rainfall patterns and stages.

Rainfall intensity (mm/h)	Rainfall pattern	Rainfall stage	V（cm/s）		Re		Fr		f	
			NT	IT	NT	IT	NT	IT	NT	IT
30	RR	1	5.45	6.50	93.50	127.47	0.45	0.50	10.45	8.37
	FR	5	5.58	6.48	110.57	127.15	0.42	0.49	11.51	8.44
	RFR	1	5.54	6.03	62.95	78.35	0.56	0.57	6.70	6.47
	RFR	5	5.63	6.44	62.95	78.36	0.57	0.62	6.39	5.31
	FRR	3	5.77	6.49	122.79	137.05	0.42	0.48	11.57	9.05
60	RR	2	6.82	7.60	93.53	127.50	0.62	0.63	5.32	5.26
	FR	4	7.12	7.97	110.61	127.19	0.61	0.67	5.54	4.54
	RR	3	8.48	9.81	93.55	127.54	0.86	0.92	2.77	2.44
	FR	3	8.92	10.62	110.64	127.24	0.86	1.04	2.82	1.92
	RFR	2	8.24	10.11	62.97	78.39	1.01	1.23	2.03	1.37
	RFR	4	9.14	9.71	62.95	78.38	1.06	1.18	1.85	1.49
	FRR	2	9.42	10.14	122.88	137.15	0.88	0.93	2.65	2.38
90	FRR	4	9.82	10.95	122.89	137.16	0.94	1.05	2.34	1.89
	CR	1	8.80	10.93	97.72	101.52	0.89	1.21	2.59	1.40
	CR	2	9.34	12.96	97.73	101.53	0.98	1.57	2.16	0.84
	CR	3	8.58	13.14	97.72	101.53	0.86	1.60	2.80	0.81
	CR	4	8.87	12.52	97.72	101.53	0.90	1.49	2.53	0.93
	CR	5	9.15	11.45	97.72	101.52	0.95	1.30	2.30	1.22
120	RR	4	11.53	13.90	93.57	127.59	1.37	1.55	1.10	0.86
	FR	2	11.99	13.70	110.67	127.27	1.33	1.52	1.16	0.89
	RR	5	14.41	18.56	93.59	127.61	1.91	2.40	0.57	0.36
	FR	1	14.19	18.01	110.69	127.30	1.72	2.29	0.70	0.39
150	RFR	3	13.37	16.83	62.99	78.41	2.09	2.64	0.48	0.30
	FRR	1	13.06	16.11	122.92	137.21	1.44	1.87	1.00	0.59
	FRR	5	14.69	19.36	122.93	137.23	1.72	2.46	0.70	0.34

Note: V, mean flow velocity; Re, Reynold number; Fr, Froude number; f, Darcy–Weisbach friction coefficient.

The RDA biplot illustrates how surface runoff and sediment yield correlate with rainfall intensity and hydraulic parameters (Figure 6). Under the IT treatment, runoff volume and sediment concentration accounted for 50.70% and 3% of the total variance, respectively. The first axis, accounting for 50.85% of the variation, was primarily associated with rainfall intensity, Fr, V, and f, while the second axis (2.88%) was driven only by rainfall stage and Re. Although the angle of the arrow was sharp among Fr, V, rainfall intensity, runoff volume, and sediment concentration, the

angle between f and other variables was greater than 90°. In addition, the length of the arrow for Re and rainfall stage was obviously shorter than that of the other variables and lies on the second axis. The NT treatment followed a similar pattern to the IT treatment between different variables. The correlation analysis further indicated that the runoff volume and sediment concentration were extremely significantly correlated with rainfall intensity and hydraulic parameters (V, Fr, and f) for both IT and NT ($P < 0.01$), in which there was a positive correlation between surface runoff and sediment yield with V, Fr, and rainfall intensity, but a negative correlation was observed with f (Figure 6). The results suggested that V, Fr, and rainfall intensity increased with increasing soil and water loss, while f decreased with increasing soil and water loss, irrespective of IT and NT. It is worth noting that the rainfall stage and Re were not significantly correlated with runoff and sediment yield ($P > 0.05$). Overall, our analysis showed that the impacts of rainfall stage on soil and water loss depended mainly on rainfall intensities and tillage intensities.
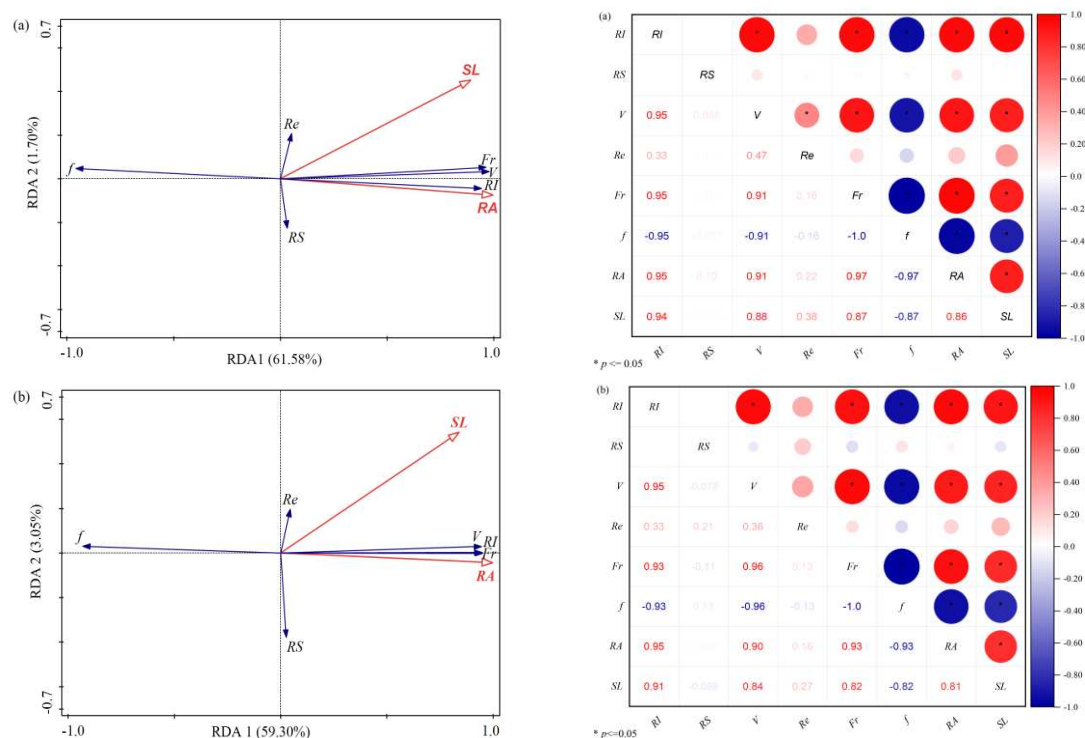
Figure 6. (A) Redundancy analysis (RDA) and (B) Correlation matrix for rainfall intensity (RI), rainfall stage (RS), V, Re, Fr, f, surface runoff (RA), and sediment yield (SL), (a) NT and (b) IT. Variance percentages explained by the RDA axes are indicated in parentheses.

To examine this result further, the surface runoff and sediment yield produced by the same rainfall intensity among different rainfall patterns are compared in Table 3. According to Table 3, the runoff volume from the different rainfall intensities was in the range of 17.90–281.90 L, with an average of 132.66 L, and 10.56–274.09 L, with an average of 119 L for IT and NT, respectively. The sediment yield produced ranged from 0.05 to 8.84 kg for IT and from 0.03 to 6.64 kg for NT. These data demonstrate that intensive tillage operations play a major role in increasing soil and water loss on landscapes with steep slopes. When the rainfall intensity increased from 30 to 150 mm h^{-1}, the average surface runoff and sediment yield increased for both NT and IT regardless of the rainfall stage or pattern, while no clear trend was found among the different rainfall patterns. It was observed that the sediment yield from the same rainfall intensity was significantly impacted by different rainfall stages and patterns. The highest sediment yields were 8.84 and 6.64 kg for IT and NT, respectively, and these were produced when the 150 mm h^{-1} intensity occurred at stage 1 in the FRR for IT and at stage 1 in the FR for NT. When comparing sediment yield values in stage 1, it can be seen that in all rainfall patterns, sediment yield was enhanced with reducing rainfall intensity. This finding suggests that the impacts of rainfall stage on soil and water loss depended mainly on rainfall intensity.

A contribution rate defined as the ratio of surface runoff to sediment yield was employed in this study to evaluate the net contributions of intensive tillage operation on soil and water loss for each rainfall intensity and stage (Table 3). From these findings, it is clear that the net influence of tillage erosion on surface runoff and sediment yield decreased with increasing rainfall intensity on sloping farmland. The contributions of intensive tillage to surface runoff and sediment yield were approximately 15.09% (range 2.77%–46.39%) and 34.48% (range 10.14%–78.95%), respectively, among the different rainfall patterns. The results displayed a decreasing trend of average contribution rate for soil loss among the five intensities, with 54.42% for 30 mm/h, 50.60% for 60 mm/h, 31.92% for 90 mm/h, 19.73% for 120 mm/h, and 19.61% for 150 mm/h, and the change tendency of surface runoff was much more similar to that of sediment yield. This result indicates that intensive tillage produces more serious soil loss than no-tillage operation.

Table 3. Comparison of runoff amount and soil loss for the same rainfall intensity with different rainfall patterns and stages.

Rainfall intensity (mm/h)	Rainfall pattern	Rainfall stage	Surface runoff (L)			Sediment yield (kg)		
			NT	IT	Contribution rate (%)1	NT	IT	Contribution rate (%)2
30	RR	1	16.15	20.61	21.64	0.04	0.19	78.95
	FR	5	19.91	34.58	42.42	0.19	0.63	69.84
	RFR	1	13.51	25.20	46.39	0.03	0.05	40.00
	RFR	5	23.67	32.14	26.35	0.06	0.12	50.00
	FRR	3	10.56	17.90	41.01	0.08	0.12	33.33
60	RR	2	55.97	70.48	20.59	0.41	0.80	48.75
	FR	4	62.44	76.01	17.85	0.68	1.43	52.45
	RR	3	118.08	133.08	11.27	1.37	1.76	22.16
	FR	3	112.72	133.34	15.46	2.12	3.11	31.83
	RFR	2	130.67	146.20	10.62	2.85	3.84	25.78
	RFR	4	133.60	156.83	14.81	1.04	1.51	31.13
	FRR	2	109.10	115.80	5.79	2.09	2.71	22.88
90	FRR	4	132.11	136.45	3.18	1.74	2.17	19.82
	CR	1	96.75	112.33	13.87	2.59	5.56	53.32
	CR	2	130.40	135.67	3.88	1.46	3.23	54.84
	CR	3	127.46	141.36	9.83	1.12	1.76	36.39
	CR	4	129.30	138.55	6.67	1.08	1.51	28.62
	CR	5	129.69	136.88	5.25	1.08	1.43	24.40
120	RR	4	162.40	182.47	11.00	2.76	3.24	14.81
	FR	2	168.20	182.23	7.70	3.70	4.91	24.64
	RR	5	239.31	254.74	6.06	3.99	4.44	10.14
	FR	1	188.63	215.20	12.35	6.64	7.92	16.16
150	RFR	3	274.09	281.90	2.77	5.55	6.40	13.28
	FRR	1	196.51	231.65	15.17	5.56	8.84	37.10
	FRR	5	193.88	204.91	5.38	3.72	4.73	21.35

Note: 1Contribution rate is the ratio of (RunoffIT − Runoff NT) to RunoffIT. 2Contribution rate is the ratio of (Soil lossIT − Soil lossNT) to Soil lossNT.

3.5. The relationship between the sediment yield rate and surface runoff rate under different rainfall patterns

The sediment yield rate (Y) was a function of the surface runoff rate (X) for the varying-intensity rainfall patterns, and their relationship can be well described with the linear equation:

$$Y = a\,X + b \qquad\qquad (1)$$

where Y is the sediment yield rate (g m^{-2} min^{-1}), X is the runoff rate (L min^{-1}), a is a regression coefficient (g m^{-2} L^{-1}) describing soil erodibility, and b is also a regression coefficient (g m^{-2} min^{-1}).

Table 4. Relationship between the runoff rate and the sediment yield rate under different rainfall patterns.

Treatment	Rainfall patter	Function equation	R2	P

	RR	Y = 1.8518 X - 3.9866	0.9398	<0.01
	FR	Y = 3.3914 X - 8.9665	0.6984	<0.01
NT	CR	Y = 0.6694 X + 5.2242	0.0.024	> 0.05
	RFR	Y = 2.1043 X - 3.6960	0.9353	<0.01
	FRR	Y = 2.6704 X - 5.4911	0.6389	<0.01
	RR	Y = 1.8797 X - 3.3415	0.9391	<0.01
	FR	Y = 3.8256 X - 10.8770	0.7786	<0.01
IT	CR	Y = 0.5210 X + 16.8220	0.0042	> 0.05
	RFR	Y = 2.4398 X - 5.6022	0.8704	<0.01
	FRR	Y = 3.4213 X - 10.4310	0.7602	<0.01

Note: X is the surface runoff rate (L min^{-1}), Y is the sediment yield rate (g m^{-2} min^{-1}).

The analysis showed that the sediment yield rate was significantly and linearly correlated with the runoff rate for each rainfall event ($P < 0.05$), yet there was no significant linear relationship between the sediment yield rate and runoff rate under CR for both the NT and the IT treatments ($P > 0.05$). The descriptive coefficients a and b of the regression equations showed different variation features of soil and water loss between the NT and IT treatments under different rainfall patterns (Table 4), implying that the significant impact of the rainfall pattern on soil and water loss was influenced by different tillage intensities. The values of coefficient a were larger for IT than for NT under the same rainfall patterns. This result shows that intensity of tillage exerts a critical effect on surface runoff and sediment yield in sloping landscapes.

4. Discussion

There are greater runoff-initiating times and cumulative sediment production under FR and FRR compared with those for the other rainfall patterns. These results are in accordance with the conclusions of Wang et al. (2017) [2], who reported that earlier high-intensity precipitation sequences produced larger soil and water losses. One explanation is that surface runoff is quickly generated in the initial stage of rainfall under FR and FRR due to a heavy rainfall intensity of 150 mm h–1 lasting for 12 min and 10.60 min, respectively. Another explanation is that when the heavy rainfall intensity appears in the early stage of rainfall, the soil moisture content rapidly reaches saturation, and a large amount of rainfall does not have time to infiltrate. Furthermore, rainfall mixes with loose soil particles on the slopes to form a slurry, which blocks the soil air from escaping the void, greatly reducing the infiltration rate. The extent of soil loss on steep slopes can be exacerbated by water accumulation and downslope rainfall flow, as well as by the movement of soil particles, when infiltration is limited during the rainfall event [27]. The third potential reason is that the surface of bare soils is very apt to form soil crusts or seals due to the fine particles being splashed by raindrops; this scenario would block soil pores under a high-intensity rainfall event [28]. Soil loss was found to be greater on crusted surfaces due to both higher runoff volume and lower hydraulic resistance, regardless of the specific scenario. Fox et al. (2004) and Marzen et al. (2020) similarly noted that intensive tillage can significantly increase erosion by bringing loose sediments to the surface [29, 30]. In this context, soils caused by tillage that accumulate at lower slope positions can be easily carried away during high-intensity rainfall events, as there may be no bank to retain them. Heavy rainfall can cause a soil crust or seal to form, leading to increased runoff and potentially triggering soil erosion. This is because the crust has a decreased permeability and a lower infiltration rate than that of the underlying soil, and the finer pores may exacerbate the effects of erosion.

SEM showed that the RI and RP had positive association with RA and SL and there was no association between RI and RP (Figure 7). The RI and RP directly affected V, Re, Fr and indirectly affected f for both NT and IT, in addition, V, Re and f directly affected SL irrespective of tillage intensive. The relationship between the sediment yield rate and surface runoff rate for varying-intensity rainfall patterns was modelled using a linear equation. These results support the findings

of Wang et al. (2014), who observed a positive correlation between sediment yield rate and runoff rate on bare soil [31]. However, these results are inconsistent with previous research that found a negative relationship between sediment yield rate and runoff rate on shrub land and grass plots [26, 32]. In our study, sediment production increased with increasing runoff volume, which may be attributed to the increased transport capacity for carrying detached sediment as runoff volume increases on bare soils, regardless of NT and IT, due to the lack of a barrier that can stop surface runoff on slopes. Previous research has shown that vegetation coverage can effectively decrease soil and water loss on hillslopes [33]. Additionally, the correlation between runoff rate and sediment yield rate is often used as an indicator of soil erodibility, with the slope of the regression equation (the regression coefficient a) considered a critical parameter of soil erodibility [31]. The values of a between the NT and IT treatments were different, with larger values for the IT treatment and lower values for the NT treatment. This result is consistent with previous research indicating that increased tillage erosion leads to an increase in soil erodibility [17, 34]. This difference primarily results from the distinctly different soil texture and thickness of soil profiles on the upper slope positions between the two tillage treatments. Long-term tillage can alter soil texture, leading to variable soil erodibility. Tillage erosion is a gradual process of downslope transport resulting from consecutive and intense tillage that can cause notable changes in soil properties, adversely influencing soil structure [12]. Furthermore, sediments deposited by intense tillage contained more fine particles and rock fragments than did non-tilled soil. Under these conditions of tillage-caused finer fragmentation, the intensity of tillage erosion is directly linked to soil erodibility on sloping farmland [35].
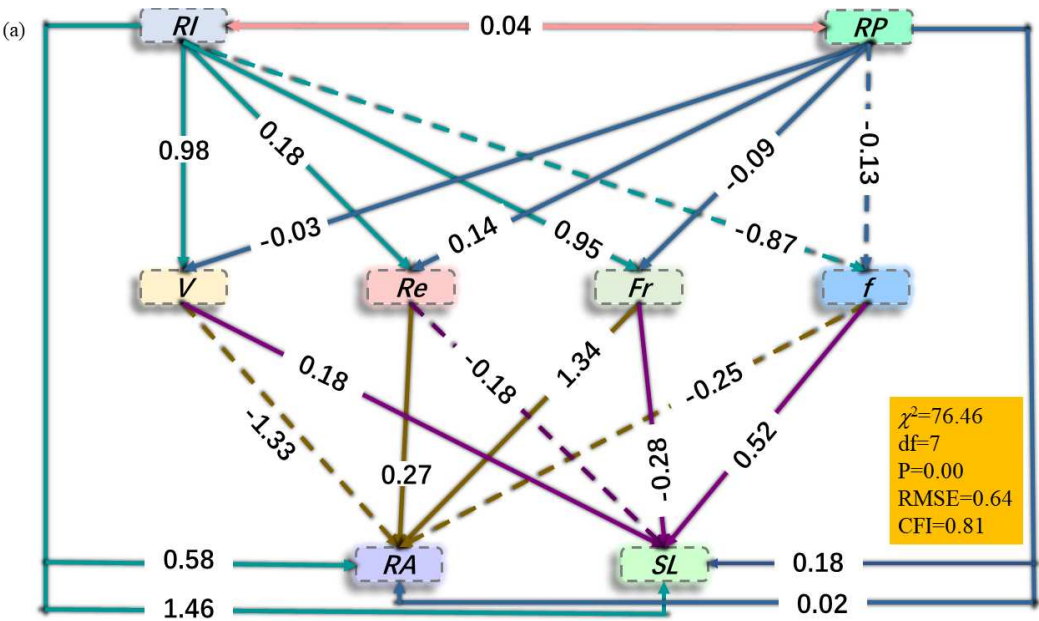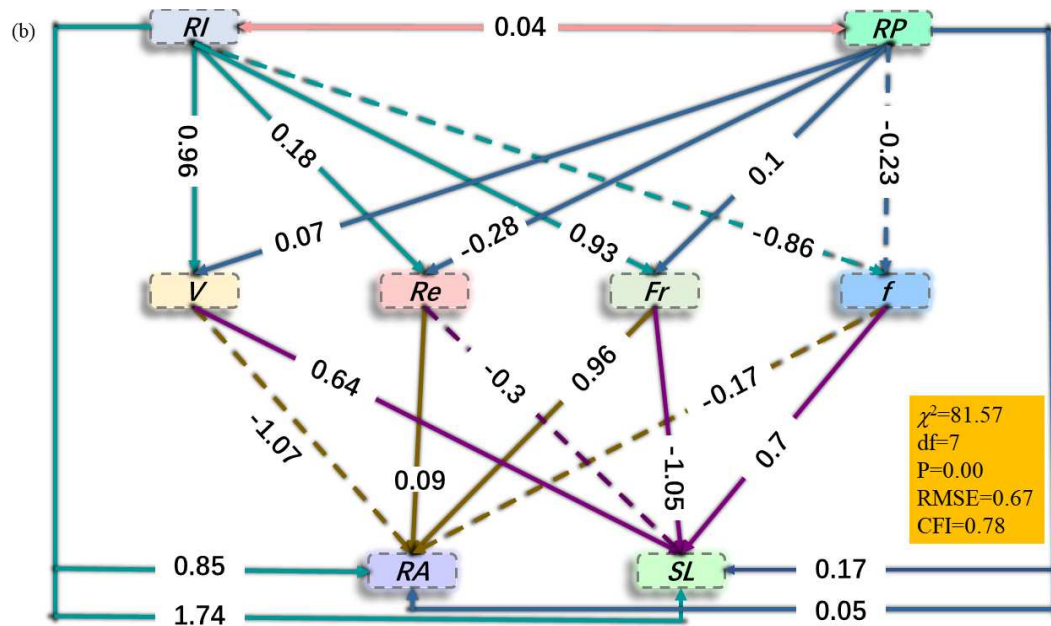
Figure 7. Structural equation model (SEM) showing the effects of rainfall intensity (RI) and rainfall pattern (RP) on surface runoff (RA), and sediment yield (SL), (a) NT and (b) IT. Solid and dashed lines show positive and negative correlations, respectively. Numbers beside arrows indicate standardized coefficients.

Tillage operation in agricultural systems can significantly alter the geomorphology of the landscape by moving soil from upper slope positions to lower ones, resulting in faster and more variable changes in soil thickness. Long-term tillage has led to thinner topsoil layers at upper slope positions, thus reducing soil infiltration and water-holding capacity [36]. As a result, soils at upper slope positions reach saturation points sooner than those at middle and lower positions, leading to saturation-excess overland flow that converges at lower slope positions [11, 37]. This process has been demonstrated as the dominant soil hydrological process in areas with a shallow soil depth [38, 39], and the process triggers greater soil and water losses at lower slope positions than in the thick soil layers at upper slope positions. Due to thin soil profiles at upper slope positions, the impeding layer to infiltrating water appeared to be the bedrock, which has a faster flow velocity and stronger water conductivity. This leads to vertical infiltrating water being turned to the downslope direction when it reaches the soil-bedrock interface and forms soil interflow, moving in the line of slope [12]. This condition (thin soil layer caused by tillage erosion at summit positions) can significantly exaggerate soil and water losses on hillslopes.

Compared with the no-tillage operation, intensive tillage erosion can significantly accelerate soil loss by carrying surface runoff, decreasing infiltration rates and intercepting sediment matter. The explanation for these findings was that severe erosion by tillage can completely remove the Ap horizons, especially in the upper slope positions. The thickness of topsoil horizons decreases significantly with an increase in soil erosion caused by long-term tillage operation, resulting in a reduction in the total depth of the soil profile [17, 21]. Intensive tillage erosion can expose bedrock in summit positions, which is an extreme phenomenon that occurs in the cultivated soils of purple regions and has crucial implications for soil and water loss. Soil erosion causes the upper horizons to be shortened and the subsurface horizons to be exposed, resulting in a rapid reduction in organic matter and nutrients, as well as a decline in the physical properties of the soil near the surface [40]. Tillage operations can cause irreversible damage to soils with shallow surface layers through soil erosion. The surface soil plays a crucial role in dividing rainfall into various hydrological components and regulating surface runoff. As a result, the loss of topsoil leads to a reduction in the soil's capacity to retain water and nutrients. Furthermore, the exposure of subsurface horizons increases the risks of surface runoff and soil loss due to decreased soil structural development and weak anti-erodibility [41, 42]. Additionally, tillage-induced erosion can lead to the exposure of subsurface horizons that have distinct properties compared to the uneroded topsoil, frequently possessing fragile and unfavourable structural features. Eroded soils are more susceptible to surface sealing and crust

formation under the impact of raindrops, causing a reduction in water infiltration and affecting soil structural development. As a consequence, soil and water loss by rainfall was exaggerated by intensive tillage on sloping farmland.

This study highlights the significant impact of variations in rainfall patterns on surface runoff and sediment yield occurrence on tilled slopes. However, it is difficult to reliably predict the influences of different tillage methods (e.g., contour tillage and upslope tillage) on soil erodibility and hydrological properties due to our limited experiments. Further research is necessary to examine the correlation between tillage erosion processes and rainfall patterns in mechanized agriculture areas. This information will be crucial in identifying ecological hazards and developing effective management strategies to address the significant threat that soil erosion poses to our land resources.

5. Conclusion

Artificial rainfall events with the same total rainfall of 90 mm and different sequences of rainfall intensities were applied to steel tanks (2 m × 5 m) to examine the impacts of rainfall patterns on surface runoff and sediment yield and to quantify the net contributions of intensive tillage on soil and water loss in the purple soil area of China. Differences in surface runoff and soil loss were found to be significant across various rainfall patterns and stages. Soil loss by intensive tillage erosion exhibited obvious differences among the five different rainfall patterns in this study, with the following order: FRR > FR > RFR> CR > RR, and the result largely depended on the heavy rainfall sequences during an event, showing that the intensive tillage erosion influences on soil and water losses are closely related to the rainfall patterns. The average contributions of intensive tillage to surface runoff and soil loss were 15.09% and 34.48%, respectively. Compared with the no-tillage treatment, the cumulative sediment production by intensive tillage erosion increased by an average of 41.24% (range 21.69%–83.95%) under the different rainfall patterns, indicating that soil loss by rainfall events was exaggerated because of tillage erosion on steep slopes. Surface runoff and soil loss were positively correlated with V and Fr but negatively correlated with f regardless of tillage intensity. The results suggest that the combination of intensive tillage erosion and varying rainfall patterns can lead to alterations in soil hydrological characteristics, ultimately resulting in poor water-holding capacity. Specifically, the thin soil layers caused by intensive tillage erosion at upper slope positions may increase overland water flow, contributing to water erosion and potential soil and water loss.

Author Contributions: Y.W.: conceptualization, methodology, writing—original draft. J.W. and Z.M. review and editing. X.L. and X.L.: resources, writing—review and editing, supervision. Y.J.: data curation and investigation. All authors have read and agreed to the published version of the manuscript.

Declaration of Competing Interest: The authors declare that there is no conflict of interest in this paper.

Data availability: Data will be made available on request to the corresponding author.

Conflicts of Interest: The authors declare no conflict of interest. The funders had no role in the design of the study; in the collection, analyses, or interpretation of data; in the writing of the manuscript; or in the decision to publish the results.

References

1.   Petan, S.; Rusjan, S.; Vidmar, A.; Mikoš, M. The rainfall kinetic energy–intensity relationship for rainfall erosivity estimation in the Mediterranean part of Slovenia. J. Hydrol. 2010, 391(3–4): 314–321. https://doi.org/10.1016/j.jhydrol.2010.07.031

2.   Wang, B.; Steiner, J.; Zheng, F.; Gowda, P. Impact of rainfall pattern on interrill erosion process. Earth Surf. Process. Land. 2017, 42(12), 1833–1846. https://doi.org/10.1002/esp.4140

3.   Meshesha, D.T., Tsunekawa, A.; Tsubo, M.; Haregeweyn, N.; Tegegne, F. Evaluation of kinetic energy and erosivity potential of simulated rainfall using Laser Precipitation Monitor. Catena 2016,137: 237–243. https://doi.org/10.1016/j.catena.2015.09.017

4.   Alavinia, M.; Saleh, F.N.; Asadi, H. Effects of rainfall patterns on runoff and rainfall-induced erosion. Int. J. Sediment Res. 2019, 34(3), 270–278. https://doi.org/10.1016/j.ijsrc.2018.11.001

5.   Dunkerley, D.L. Rain event properties in nature and in rainfall simulation experiments: a comparative review with recommendations for increasingly systematic study and reporting. Hydrol. Process. 2008, 22(22): 4415–4435. https://doi.org/10.1002/hyp.7045

6.   Mohamadi, M.A.; Kavian, A. Effects of rainfall patterns on runoff and soil erosion in field plots. Int. Soil Water Conserv. Res. 2015, 3, 273–281. http://dx.doi.org/10.1016/j.iswcr.2015.10.001

7.   Zheng, F.; Bian, F.; Lu, J.; Qin, C.; Xu, X. Effects of rainfall patterns on hillslope erosion with longitudinal ridge in typical black soil region of Northeast China. Trans. CSAM 2016, 47(2): 90 － 97. https://doi.org/10.6041/j.issn.1000-1298.2016.02.013

8.   An, J.; Yu, Y.; Wu, Y. Effects of rainfall patterns on hillslope soil erosion process of cinnamon soil in contour ridge system. Trans. CSAE 2017, 33(24): 150－156. 10.11975/j.issn. https://doi.org/1002-6819.2017.24.020

9.   Dunkerley, D. Effects of rainfall intensity fluctuations on infiltration and runoff: Rainfall simulation on dryland soils, Fowlers Gap, Australia. Hydrol. Process. 2012, 26, 2211–2224. https://doi.org/10.1002/hyp.8317

10. Wang, L.; Dalabay, N.; Lu, P.; Wu, F. Effects of tillage practices and slope on runoff and erosion of soil from the Loess Plateau, China, subjected to simulated rainfall. Soil Tillage Res. 2017a, 166, 147–156. https://doi.org/10.1016/j.still.2016.09.007

11. Govers, G.; Quine, T.A.; Desmet, P.J.J.; Walling, D.E. The relative contribution of soil tillage and overland flow erosion to soil redistribution on agricultural land. Earth Surf. Process. Landf. 1996, 21, 929–946. https://doi.org/10.1002/(SICI)1096-9837(199610)21:10<929::AID-ESP631>3.0.CO;2-C

12. Zhang, J.H.; Jia, L.Z.; Wang, Y.; Zhang, Z.H. Tillage erosion effect on soil hydrological properties in a hilly landscape. J. Hydrol. Eng. 2017, 22(9), 04017034. https://doi.org/10.1061/(ASCE)HE.1943-5584.0001565

13. Kumar, S.; Kadono, A.; Lal, R.; Dick, W. Long-term tillage and crop rotations for 47–49 years influences hydrological properties of two soils in Ohio. Soil Sci. Am. J. 2012, 76(6), 2195-2207. https://doi.org/10.2136/sssaj2012.0098

14. Biddoccu, M.; Ferraris, S.; Pitacco, A.; Cavallo, E. Temporal variability of soil management effects on soil hydrological properties, runoff and erosion at the field scale in a hillslope vineyard, North-West Italy. Soil Tillage Res. 2017, 165, 46–58. https://doi.org/10.1016/j.still.2016.07.017

15. Abdi, E.; Saleh, H.R.; Majnonian, B.; Deljouei, A. Soil fixation and erosion control by Haloxylon persicum roots in arid lands, Iran. J. Arid Land, 2019, 11, 86–96. https://doi.org/10.1007/s40333-018-0021-2

16. Vanacker, V.; Ameijeiras-Mariño, Y.; Schoonejans, J.; Cornélis, J. T.; Minella, J.P.; Lamouline, F.; ... & Opfergelt, S. Land use impacts on soil erosion and rejuvenation in Southern Brazil. Catena 2019, 178, 256–266. https://doi.org/10.1016/j.catena.2019.03.024

17. Wang, Y.; Zhang, J.H.; Zhang, Z.H. Influences of intensive tillage on water-stable aggregate distribution on a steep hillslope. Soil Tillage Res. 2015, 151, 82–92. https://doi.org/10.1016/j.still.2015.03.003

18. Cheik, S.; Bottinelli, N.; Soudan, B.; Harit, A.; Chaudhary, E.; Sukumar, R.; Jouquet, P. Effects of termite foraging activity on topsoil physical properties and water infiltration in Vertisol. Appl. Soil Ecol. 2019, 133, 132–137. https://doi.org/10.1016/j.apsoil.2018.10.001

19. Soil Survey Staff. Keys to Soil Taxonomy. eighth ed. U.S. Gov. Print. Office, Washington, DC. 1994.

20. Liu, G.S. Soil Physical and Chemical Analysis and Description of Soil Profiles. Beijing: Chinese Standard Press 1996.

21. Zhang, J.H.; Nie, X.J.; Su, Z.A. Soil profile properties in relation to soil redistribution by intense tillage on a steep hillslope. Soil Sci. Am. J. 2008, 72(6), 1767–1773. https://doi.org/10.2136/sssaj2007.0228

22. Dai, J.; Zhang, J.; Xue, K.; Li, M.; Huang, F.; Yang, F.; Zhao, H.; Xu, Y.; Dai, C.; Ma, X. Effects of subsurface rock fragment layers caused by simulated hoeing on near-surface rainfall-runoff processes. Soil Tillage Res. 2023, 226, 105594. https://doi.org/10.1016/j.still.2022.105594

23. Dai, Q.H.; Peng, X.D.; Zhi, Y.; Zhao, L.S. Runoff and erosion processes on bare slopes in the Karst Rocky Desertification Area. Catena 2017, 152, 218–226. https://doi.org/10.1016/j.catena.2017.01.013

24. Parsons, A.J.; Stone, P.M. Effects of intra-storm variations in rainfall intensity on interrill runoff and erosion. Catena 2006, 67(1): 68–78. https://doi.org/10.1016/j.catena.2006.03.002

25. Horton, R.E.; Leach, H.R.; Van Vliet, R. Laminar sheet-flow. Eos, Transactions American Geophysical Union 1934, 15(2), 393–404. https://doi.org/10.1029/TR015i002p00393

26. Pan, C.; Shangguan, Z. Runoff hydraulic characteristics and sediment generation in sloped grassplots under simulated rainfall conditions. J. Hydrol. 2006, 331(1–2), 178–185. https://doi.org/10.1016/j.jhydrol.2006.05.011

27. Ma, W.; Li, Z.; Ding, K.; Huang, J.; Nie, X.; Zeng, G.; Wang, S.; Liu, G. Effect of soil erosion on dissolved organic carbon redistribution in subtropical red soil under rainfall simulation. Geomorphology 2014, 226, 217–225. https://doi.org/10.1016/j.geomorph.2014.08.017

28. Assouline, S.; Ben-Hur M. Effects of rainfall intensity and slope gradient on the dynamics of interrill erosion during soil surface sealing. Catena 2006, 66(3): 211–220. https://doi.org/10.1016/j.catena.2006.02.005

29. Marzen, M.; Kirchhoff, M.; Marzolff, I.; Aït Hssaine, A.; Ries, J.B. Relative quantification of wind erosion in argan woodlands in the Souss Basin, Morocco. Earth Surf. Process. Landf. 2020, 45(15), 3808–3823. https://doi.org/10.1002/esp.5002

30. Fox, D.M.; Bryan, R.B.; Price, A.G. The role of soil surface crusting in desertification and strategies to reduce crusting. Environ. Monit. Assess. 2004, 99, 149–159. https://doi.org/10.1007/s10661-004-4015-5

31. Wang, G.; Wu, B.; Zhang, L.; Jiang, H.; Xu, Z. Role of soil erodibility in affecting available nitrogen and phosphorus losses under simulated rainfall. J. Hydrol. 2014, 514, 180–191. https://doi.org/10.1016/j.jhydrol.2014.04.028

32. Abrahams, A.D.; Parsons, A. J.; Luk, S.H. Hydrologic and sediment responses to simulated rainfall on desert hillslopes in southern Arizona. Catena 1988, 15(2), 103–117. https://doi.org/10.1016/0341-8162(88)90022-7

33. Pan, C.; Ma, L. How the spatial distribution of grass contributes to controlling hillslope erosion. Hydrol. Process. 2020, 34(1), 68–81. https://doi.org/10.1002/hyp.13573

34. Van Oost, K.; Govers, G.; De Alba, S.; Quine, T. A. Tillage erosion: a review of controlling factors and implications for soil quality. Prog. Phys. Geog. 2006, 30(4), 443–466. https://doi.org/10.1191/0309133306pp487ra

35. Ni, S.J.; Zhang, J.H. Variation of chemical properties as affected by soil erosion on hillslopes and terraces. Eur. J. Soil Sci. 2007, 58 (6), 1285–1292. https://doi.org/10.1111/j.1365-2389.2007.00921.x

36. Wang, Y.; Zhang, J. H.; Zhang, Z. H.; Jia, L. Z. Impact of tillage erosion on water erosion in a hilly landscape. Sci. Total Environ. 2016, 551, 522–532. https://doi.org/10.1016/j.scitotenv.2016.02.045

37. Lobb, D.A.; Lindstrom, M.J.; Schumacher, T.E. Soil erosion processes and their interactions: implications for environmental indicators. In: Ancaviglia, R. (Ed.), Agricultural Impacts on Soil Erosion and Soil Biodiversity: Developing Indicators for Policy Analysis Proceedings OECD Expert Meeting on Soil Erosion and Soil Biodiversity. Organization for Economic Cooperation and Development, Paris, France 2004, pp. 325–336.

38. Zhu, B.; Wang, T.; Kuang, F. H.; Luo, Z. X.; Tang, J. L.; Xu, T.P. Measurements of nitrate leaching from a hillslope cropland in the central Sichuan Basin, China. Soil Sci. Am. J. 2009, 73(4), 1419–1426. https://doi.org/10.2136/sssaj2008.0259

39. Zhou, M.; Zhu, B.; Butterbach-Bahl, K.; Wang, T.; Bergmann, J.; Brüggemann, N.; Wang, Z.; Li, T.; Kuang, F. Nitrate leaching, direct and indirect nitrous oxide fluxes from sloping cropland in the purple soil area, southwestern China. Environ. Pollut. 2012, 162, 361–368. https://doi.org/10.1016/j.envpol.2011.12.001

40. Blanco, H.; Lal, R. Principles of Soil Conservation and Management. Springer, Netherlands, 2008, pp. 108–135. https://doi.org/10.1007/978-1-4020-8709-7

41. Xie, S.; Ren, W. Soil Moisture characteristics in Karst area with different land use types. Agri. Sci. Tech. 2013, 14(12), 1856. https://doi.org/10.16175/j.cnki.1009-4229.2013.12.012

42. Liu, H.; Dai, J.; Xu, C.; Peng, J.; Wu, X.; Wang, H. Bedrock-associated belowground and aboveground interactions and their implications for vegetation restoration in the karst critical zone of subtropical Southwest China. Progress Phys. Geogr. Earth Environ. 2021, 45(1), 7–19. https://doi.org/10.1177/0309133320949865